Open Access
Published Online First: September 2022

Baghdad Science Journal
2023, 20(2): 460-468

P-ISSN: 2078-8665
E-ISSN: 2411-7986

DOI: http://dx.doi.org/10.21123/bsj.2022.7036

Equilibrium, Kinetic, and Thermodynamic Study of Removing Methyl Orange Dye from Aqueous Solution Using *Zizphus spina-christi* Leaf Powder

Fadya F. Mohammed

Al-Rasheed University College, Biology Department, Baghdad, Iraq.
E-mail address: fadea.f@alrasheedcol.edu.iq.

Received 11/2/2022, Revised 9/5/2022, Accepted 11/5/2022, Published Online First 20/9/2022
Published 1/4/2023

Abstract:

In this study, *Zizphus spina-christi* leaf powder was applied for the adsorption of methyl orange. The effect of different operating parameters on the Batch Process adsorption was investigated such as solution pH (2-12), effect of contact time (0-60 min.), initial dye concentration (2-20 mg/L), effect of adsorbent dosage (0-4.5 g) and effect of temperature (20-50°C). The results show a maximum removal rate and adsorption capacity (%R= 23.146, q_e = 2.778 mg/g) at pH = 2 and equilibrium was reached at 40 min. The pseudo-second-order kinetics were found to be best fit for the removal process (R^2 = 0.997). Different isotherm models (Langmuir, Freundlich, Dubini-Radushkevich,Temkin) were applied in this study and the adsorption process was found to fit Dubinin-Radushkevich isotherm (R^2 = 0.970). The thermodynamic parameters: ΔG°, ΔH°, ΔS° were also invested, the results indicate the process to be exothermic (ΔH° = -100.933 kJ/mole), non-spontaneous, and more feasible at lower operating temperatures, with a decrease in the randomness at the solid-liquid interface (ΔS° = - 0.370 kJ/mole.K)

Keywords: Adsorption, Dubinin-Radushkevich isotherm, Methyl orange, Pseudo-second-order, Thermodynamic parameters, Zizphus spina-christi leaf powder

Introduction:

In recent years, shortage in waste-free water sources began to rise as the population of countries rises, developed countries being the most affected by water contamination risk as the effluents of factories discharged directly to rivers without undergone the proper treatment due to the high cost of pretreatment[1, 2]. Dyes used in different industries such as paper, textile, cosmetic, rubber, food industries, and hospitals. These dyes have hazardous effect on human health to the extent of being cancerous especially synthetic dyes due to their complex chemical structure which resist biodegradation making them persist for long time in aqueous medium[3-5]. Over the last decades various research reported several strategies that discuss the removal of colored pollutants from effluent water like biodegradation and bio sorption, oxidation, coagulation-flocculation process and membrane separation[6-9]. Adsorption method is wieldy utilized as the purifying process for removal of dye. Activated carbon generated from agricultural residues was utilized to adsorb various sort of colors from polluted aqueous solutions. Kola nut pod was activated through both acid and base media for the decontamination of basic dyes achieving a removal percentage of (99.4% and 99.7%) for acid and base activation respectively [10]. Activated carbon produced form *Catha edulis* stem was used to adsorb malachite green dye, at pH= 10 a maximum removal was attended (98.8%) [11]. Activated carbon prepared from Ziziphus lotus stones (ACZLS) activated by H_3PO_4 was used for removing two textile dyes Basic Yellow 28 and Basic Red 46, for both dyes a maximum removal (98%) was found at pH= 8 [12]. A composite of different types of biochars was invented to serve as an adsorbent for dyes, a green biochar/iron oxide composite was produced using a facile approach involving banana peel extract and $FeSO_4$ for the removal of methylene blue achieving a maximum adsorption capacity of (862 mg/g) at operating conditions of T= 313 K, pH= 6.1 and initial methylene blue of 500 mg/L [13]; also brilliant green removal through the use of nanocomposite prepared from chitosan, results reported a removal rate of (99.5 %) of dye form the aqueous solution at pH= 7 [14]. Several limitations

affect the use of both activated carbon and composite sorbent such as production cost. Several researchers employed raw agricultural waste as a sorbent for the purification of water from textile dye effluents. Adsorption of methylene blue using leaves of date palm in powder form was investigated. The experimental data gives an indication of feasible process with a maximum adsorption capacity of (58.14 mg/g) at T = 60 ºC and pH = 6.5 [15]. Fruits peel was employed as an adsorbent for the removal of dye from aqueous solution, Rhodamine B was successfully adsorb on the surface of Raphiahookerie peel powder with 88.88% removal at adsorbent dosage of 2g/L and a maximum capacity of adsorption (666.67 mg/g) [16]. In this study, raw *Zizphus spina-christi* leaf powder was used as low cost adsorbent for the removal of synthetic methyl orange dye from the aqueous solution.

Materials and Methods:

Preparing the Adsorbent

Zizphus spina-christi leaf powder (ZSCP) were pursued from local market (Iraq-Baghdad) as its used by local people for several domestic purposes.

Preparing the Adsorbate

Synesthetic methyl orange dye supplied by Sinopharm Chemical Reagent Co., Ltd, China was used as an organic pollutant for aqueous solution. Specification for methyl orange are listed in (Table 1). Stock solution was prepared by dissolving 1 g of MO in 1000 mL volumetric flask by adding distil water.

Table 1. Specification for Methyl Orange

Compound name	Chemical Formula	Molar Mass	Chemical structure
Methyl Orange	$C_{14}H_{14}N_3NaO_3S$	327.35 g/mol.	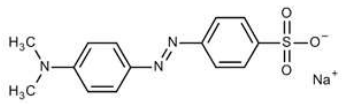

Apparatus

Uv-Vis spectrometer was used to measure the adsorption of MO by the adsorbate. The Uv-Vis was first calibrated using the different concentration prepared form MO original stock solution. The UV-Vis was set at λ_{max} = 470 nm, pH meter was used to measure and control the pH of the aqueous solution. The pH meter was calibrated using buffer solution (pH = 4,10,12). Magnetic stirrer with heating was also used to mix the content of each experiment at different time and temperature.

Adsorption Process

Batch adsorption process was performed to study the adsorption of MO on raw *Zizphus spina-christi* leaf powder. 100 ml of MO solution was placed in 250 ml beaker. The effect of pH, time, adsorbent dosage, dye concentration and temperature were investigated in the current study. The amount of dye adsorbed, q_t, at any time, t, was calculated using eq. 1

$$q_t = \frac{(C_i - C_t)}{W} * V \qquad 1$$

Where q_t(mg/g) = amount of dye adsorbed at any time

C_i = initial dye concentration (mg/L) at time = 0

C_t= dye concentration (mg/L) at any time

W= weight of adsorbent (g)

V= volume of dye solution (mL)

Rate of adsorption was determined by calculating the percentage of the removal using eq. 2

$$\%\,Removal = \frac{C_i - C_t}{C_i} * 100 \qquad 2$$

To study the adsorption of MO on ZSCP, a series of batch experiments under different operating condition were conducted. The effect of solution pH on removal process was investigated by varying the pH values (2, 3, 4, 6, 8, 10 and 12). To adjust the pH (0.1N) NaOH and (1N) HCl was added to the experiment solution. A range of different contact time experiments (0-60 min) while holding other parameters as constant (pH = 2, initial dye concentration = 12 mg/L, adsorbent dosage = 0.1g/ 100 ml solution, temperature = 20 ºC, agitation speed at 60 rpm). Different initial dye concentrations of MO solution (2-20 mg/L) were prepared by diluting the original stock of (1g/L) concentration. Adsorbent dosage (0.1- 4.5 g) was added to 100 ml of dye solution to investigate the effect of ranging the amount of active material. The effect of temperature on the removal process was also investigated over a range of different solution temperatures (20, 30, 40, and 50 ºC).

Adsorption Kinetics and Isotherm Modeling

Adsorption Kinetics:

Pseudo first order and pseudo second order[17] kinetics were employed to study the kinetics of the adsorption process, the mathematical expression for these equations are pseudo first order

$$\ln(q_e - q_t) = \ln q_e - k_1 \qquad 3$$

where q_e and q_t are the amount of dye adsorbed in (mg/g) at equilibrium and at any time respectively, k_1 (1/ min) is rate constant of adsorption.

pseudo second order

$$\frac{t}{q_t} = \frac{1}{k_2 q_e^2} + \frac{1}{q_e t} \qquad 4$$

rate constant of the pseudo 2nd order is represented by k_2(g/mg.min) .

Isotherm Modeling:

Four different adsorption isotherms were utilized using the experimental data to investigate the best model that express the adsorption process

Langmuir Isotherm

This model proposes that the removal process follows a mono-layer molecular adsorption where each dye molecule is in contact with the active sites on the surface of the adsorbate material [12] The mathematical equation:

$$\frac{C_e}{q_e} = \frac{1}{q_m C_e} + \frac{1}{K_L q_m} \qquad 5$$

Where q_m is the maximum amount of dye begin adsorbed in mono-layer (mg/g) ,and K_L is the constant of Langmuir (L/mg) . An important parameter known as the separating factor R_L is essential in this isotherm model:

$$R_L = \frac{1}{1+K_L C_e} \qquad 6$$

R_L= 0 indicate an irreversible process, 0 < R_L< 1 indicate a favorable process, while R_L= 1 adsorption shows a liner behavior [12, 15].

Freundlich Isotherm

Instead of monolayer adsorption this model assumes a multilayer heterogeneous adsorption on adsorbate surface [16] the linearization of Freundlich isotherm is [15, 18]:

$$\log q_e = \log K_F + \frac{1}{n}\log C_e \qquad 7$$

Where K_F is constant of Freundlich ((L/mg)$^{1/n}$) and n represents the intensity of adsorption.

The Dubinin-Radushkevich (D-R) Isotherm

This isotherm gives an importance to the pore size and distributions and its effect on whole adsorption process as well as energy of adsorption which describes the process being physical or chemical in nature [2] this model is expressed mathematically by [15]:

$$\ln q_e = \ln q_m - \beta \varepsilon^2 \qquad 8$$

Where q_m is the maximum capacity of adsorption (mg/g), β (mole^2/kJ^2) is the activity constant that is related to the mean free energy of adsorption E (kJ/mole) , and Ɛ is the Polanyi potential. Both E and Ɛ can be correlated as follow:

$$\varepsilon = RT \ln\left(1 + \frac{1}{C_e}\right) \qquad 8A$$

$$E = \sqrt{\frac{1}{2\beta}} \qquad 8B$$

Where R is the universal gas constant (J/mole.K) and T the temperature in (K). The value of E determines whether the adsorption process is physical (E < 8 kJ/ mole) , chemical (8< E<16 kJ/ mole) or governed by ion-exchange mechanism (E > 16 kJ/mole) [10, 19].

Temkin Isotherm

This isotherm model focuses on the heat of adsorption and on the interaction on the surface between adsorbent-adsorbate. A liner decreases in the heat of adsorption is proposed by Temkin model as more adsorbent molecule interacts with the surface of the adsorbate, this case is valid while extremely high or low dye concentrations are ignored. Furthermore, the adsorption is represented by the bounding energy up to a maximum bounding energy [15-17] mathematically expressed as follow [16]:

$$q_e = B\ln A + B\ln C_e \qquad 9$$

$$B = \frac{RT}{b} \qquad 9a$$

Where b is the Temkin constant(J/mol) and A is the Temkin isotherm constant (L/g).

Study of Thermodynamics

To investigate whether the adsorption process is spontaneous and feasible, endo or exothermic, a series of experiment were conducted at different temperatures (20,30,40 and 50 ºC) to calculate the thermodynamic parameters: Gibb's free energy ΔGº, change of enthalpy ΔHº, and change of entropy ΔSº these parameters were calculated using the following eqs [15] :

$$\Delta G^o = -RT\ln K_d \qquad 10$$

Where K_d is thermodynamic equilibrium constant calculated form eq. 11 :

$$K_d = \frac{q_e}{C_e} \qquad 11$$

$$\ln K_d = \frac{\Delta S^\circ}{R} - \frac{\Delta H^\circ}{RT} \qquad 12$$

Values of both ΔSº and ΔHº can be calculated form the intercept and the slope of the liner plot of ln K_d vs 1/T.

Results and Discussion:

Characterization of ZSCP Surface

Morphology of ZSCP surface was studied using filed emission scanning electron microscope (FE-SEM) before and after adsorption at the same magnification power (5000x). Fig. 1A revels the

Baghdad Science Journal
2023, 20(2): 460-468
P-ISSN: 2078-8665
E-ISSN: 2411-7986

rough and heterogeneous characteristics of ZSCP surface before adsorption which provides the desired pores sites for the adsorption of MO dye molecules. Fig.1B shows a significant change in the morphology of ZSCP with a much smother surface due to the adsorption of MO dye molecules.

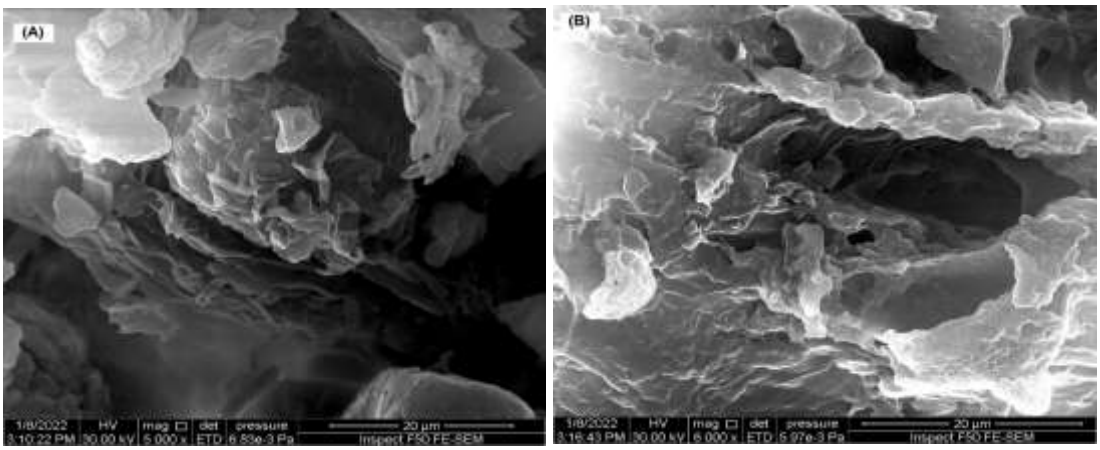

Figure 1. FE-SEM image of ZSCP surface (A) before (B) after adsorption of MO dye

Effect of solution pH

Figure 2 represents the behavior of the adsorption process at different values of solution pH. The figure clearly shows that the adsorption process is more favorable at acidic medium (pH= 2) with a maximum value of dye adsorbed of q_e= 2.777 mg/g and removal rate of 23%. According to the literature[20-22] such behavior is interpreted as follow: at low pH the amount of H^+ ions increase in the aqueous solution which causes the surface of the ZSCP to be positively charged, with the dye molecules having a negative charge a strong electrostatic force is formed between the ZCPS surface and MO molecules leading to an increase in the rate of adsorption of dye. On the contrary, as the pH value increases towards the basic medium the rate of dye adsorption decreases due to an increase in HO^- ions, the ZSCP surface becomes negatively charged and repulses the MO molecules forcing the dye to stay in the aqueous solution. These results signify the importance of solution pH on the adsorption process. According the experimental results, the optimum value of pH for the adsorption process is equal to 2.

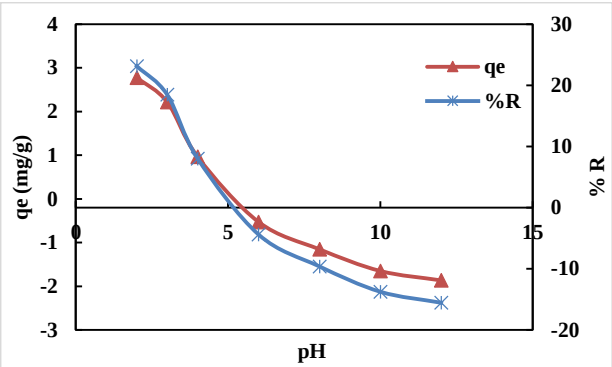

Figure 2. Effect of pH on q_e and %R of MO adsorption on ZSCP (at C_i= 12 mg/L, adsorbent dosage = 0.1 g/100 mL, temperature = 20 ºC, time = 40 min., rpm = 60)

Effect of Contact Time

Rapid increase in both amount of dye adsorbed and removal rate of dye form the aqueous solution within the first 10 minutes of the batch process as shown in Fig.3 with maximum values equal to (q_e= 3.339 mg/g, %R= 27.83 %) at time = 5 min. This was due to the presence of a greater number of accessible available active sites on the surface of ZSCP. As the contact time between the MO solution and adsorbate material increases the values of both q_e and %R starts to drop gradually due to vacant sites were almost fully occupied by dye molecules thus the efficiency of the adsorbate material decreases [21-23]. The saturation which was found to reach at time was equal to 40 min. with no significance increase in the adsorption process as contact time increases, therefore, the equilibrium time for the batch removal process was chosen to be 40 min.

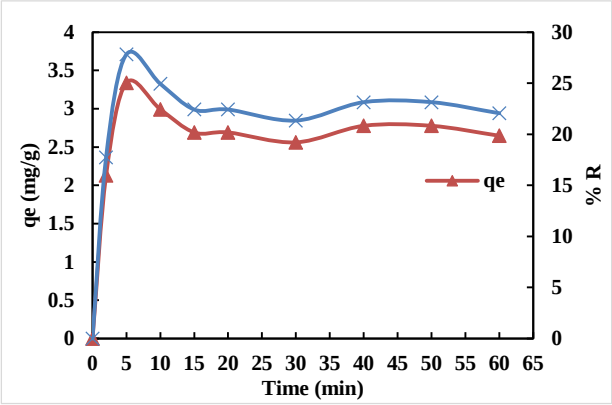

Figure 3. Effect of Contact time on q_e and % R of MO adsorption on ZSCP (at C_i= 12 mg/L, adsorbent dosage = 0.1 g/100 mL, temperature = 20 ºC, rpm = 60).

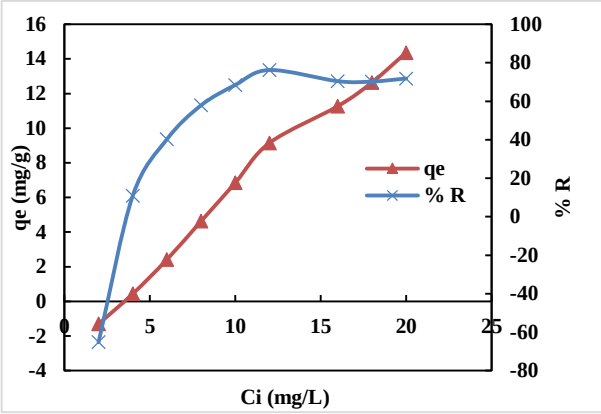

Figure 4. Effect of initial dye concentration on q_e and %R of MO adsorption on ZSCP (at C_i= 12 mg/L, pH= 2, adsorbent dosage = 0.1 g/100 mL, temperature = 20 ºC, time = 40 min., rpm = 60).

Effect of Initial Dye Concentration

Figure 4 illustrates the effect of initial dye concentration on the adsorption process. The adsorption capacity q_e continues to increase as the values of C_i increase. At the C_i = 20 mg/L (the max. initial dye concentration for the batch process) the amount of q_e is equal to 14.363 mg/g. Such behavior can be associated with the increase in the mass transfer driving force as the concentration of the dye increases in the aqueous solution which enables the dye molecules to overcome the resistance force at the solid-liquid interface and bind with pores on the surface of ZSCP [24, 25]. On the contrary, the removal rate decreases form 76.24% at Ci = 12 mg/L to 71.81 % at Ci = 20 mg/L. At lower initial dye concentration, all molecules of dye present in the solution bind with the active pore site of the adsorbate enhancing the removal process. All adsorbents, on the other hand, have a finite number of binding sites that become saturated at a particular concentration. Because of the rivalry with the active sites, not all dye molecules become adsorbed on sites, and some dye molecules remain unadsorbed, resulting in a reduction in dye removal. Bisorption of crystal violet on jackefrute leaf powder [26] and acid violet 17 dye adsorption on activated Ficus racemose leaves[27] followed a similar pattern.

Effect of Adsorbent Dosage

Figure 5 demonstrates the experimental result for varying the amount of adsorbent dosage on the values of both q_e and %R. An increase in the value of %R is evident as the amount of ZSCP in the aqueous solution increases reaching a maximum value of %R = 76.242 % at ZSCP dosage of 4 g/100mL, due to the availability of more active vacant sites as the amount of the adsorbent increases. On the contrary, the capacity of MO adsorption decreases as the dosage of ZSCP increases. Many adsorption systems have also reported such patterns as a result of the overlapping between the active sites of adsorbent themselves at high dose, resulting in a reduction in the number of effective sites on the adsorbent surface. [11, 13, 28].

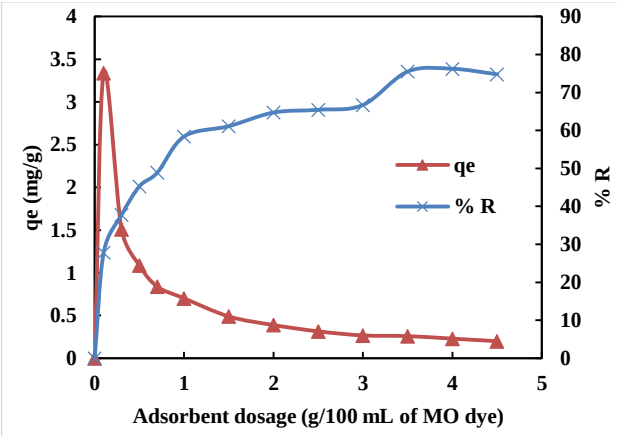

Figure 5. Effect of adsorbent dosage on q_e and %R of MO adsorption on ZSCP (at C_i= 12 mg/L, pH= 2, temperature = 20 ºC, time = 40 min. rpm = 60).

Adsorption Kinetics and Isotherm Modeling

Adsorption Kinetics

To describe the kinetics that govern the mechanism of adsorption process pseudo-first

Baghdad Science Journal
2023, 20(2): 460-468
P-ISSN: 2078-8665
E-ISSN: 2411-7986

(figure not shown) and pseudo- second orders model were applied to the experimental data. Pseudo –first order kinetics fails to give a good agreement with the experimental data. Fig.6 demonstrates the validity of pseudo-second order for describing the adsorption of MO onto ZSCP with correlation coefficient (R^2= 0.9971). Therefore, the best correlation of experimental data were by the pseudo-second order kinetic model, chemical reaction may be recognized as the rate-controlling step in the studied adsorption systems, where valency forces are involved via electron sharing or exchange between the adsorbent and the adsorbate.[29, 30]. The values for the kinetic model are listed in (Table 2).

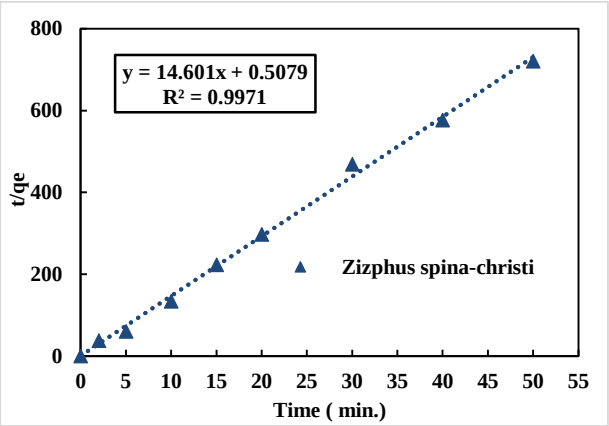

Figure 6. Adsorption Kinetics plot (pseudo-second order) of MO on ZSCP (at C_i= 12 mg/L, pH=2, adsorbent dosage=4g/100mL, temperature = 20 ºC, rpm = 60).

Table 1. Adsorption kinetics parameters of MO adsorption on ZCSP at T = 20ºC and C_i = 12 mg/L.

PSO parameters	q_e (mg/g)	K_2 (1/min)	R^2
	0.685	41.966	0.997

Isotherm Modeling:

To understand the behavior of the interaction between MO dye molecules and the ZCSP during the adsorption process, four most common isotherm models (Langmuir, Freundlich, Temkin and Dubinin-Radushkevich (D-R)) were applied to the experimental data. The process was found to fit both D-R and Temkin models and it was not valid for the other models, (Figs.7,8) represent the linearization of both models. The isotherm parameters corresponding to each model are listed in (Table 3). Comparing the values of correlation coefficients for both isotherm, the D-R model found to best describe the process (R^2 = 0.970) from the value of E one of the parameters in D-R isotherm model which represents the mean free adsorption energy, proposes a physical process might govern the adsorption of MO on the ZSCP [10, 19]. Fig.8 describes a reasonable fit for the experimental data with the Temkin model (R^2 = 0.909) the positive value of B which indicates an endothermic adsorption process[12].

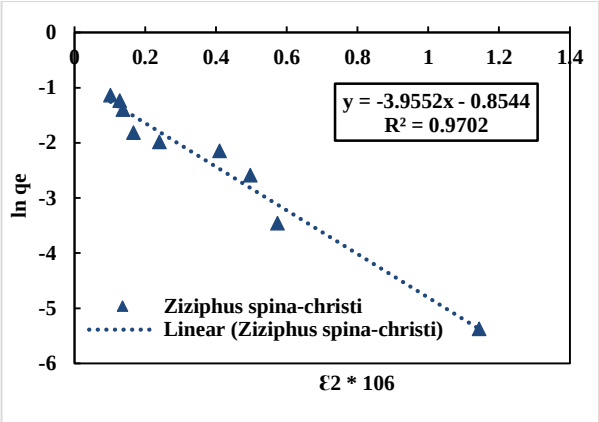

Figure 7. Dubinin-Radushkevich adsorption isotherm model of MO on ZSCP.

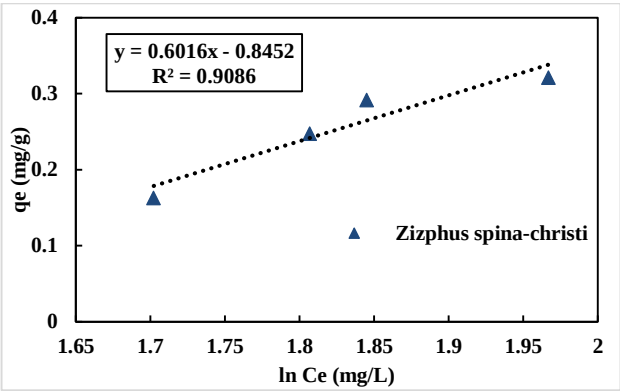

Figure 8. Timken adsorption isotherm model of MO on ZSCP.

Table 2. Adsorption isotherms parameters of MO adsorption on ZSCP

Timken isotherm	Values	D-R isotherm	Values
B_T (J/mole)	24.065	E (kJ/mole)	0.356
K_t (L/mole)	0.704	β ($mole^2/J^2$)	3.96E-09
		q_m (mg/g)	4.255
R^2	0.909	R^2	0.970

Effect of Temperature and Thermodynamic Parameters

Figure 9 illustrates the effect of varying batch process temperature, it is evident that as the temperature rises both adsorption capacity and percentage of removal decrease indicating a shift towards an exothermic process as the temperature rises, where the adsorption and removal is more favorable and endothermic at lower temperatures. An explanation for this behavior is that the adsorption forces between the MO molecules and

the surface pore of ZSCP weakened as the temperature rises which leads to the release of MO molecules from the pores into the solution [31]. Another possible explanation is the increase in the kinetic energy of the MO molecules due the increase in temperature which leads the molecules to be separated from the surface of the adsorbate leading to a decrease in the amount of dye removed for the aqueous solution [32].The thermodynamic parameters are listed in (Table 4). ΔGº values are positive indicating a non-spontaneous and more feasible at lower temperature which does not require adding an energy input to enhance the process [32-34]. Values of ΔHº and ΔSº were calculated from the slope and intercept of Fig.10. The negative ΔHº value (-100.933 kJ/mole) confirms an exothermic removal of MO where physical adsorption forces are dominated [24, 31, 32]. On the other hand, the negative value of ΔSº (-0.370 kJ/mole.K) reflects a reduction in the randomness at the solid-liquid interface during the process of adsorption [24, 31-35].

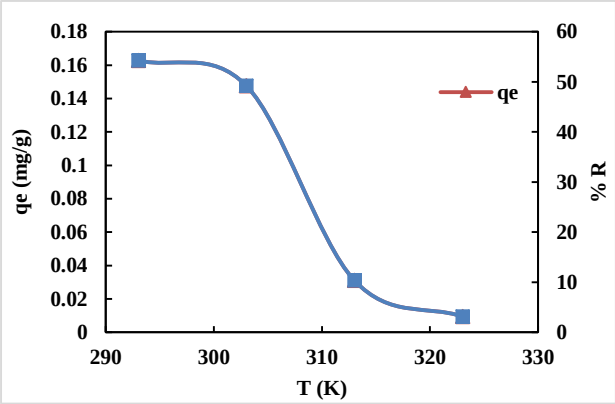

Figure 9. Effect of temperature on q_e and %R of MO adsorption on ZSCP (at C_i= 12 mg/L, pH = 2, adsorbent dosage = 4 g/100 mL, time = 40 min. , rpm = 60)

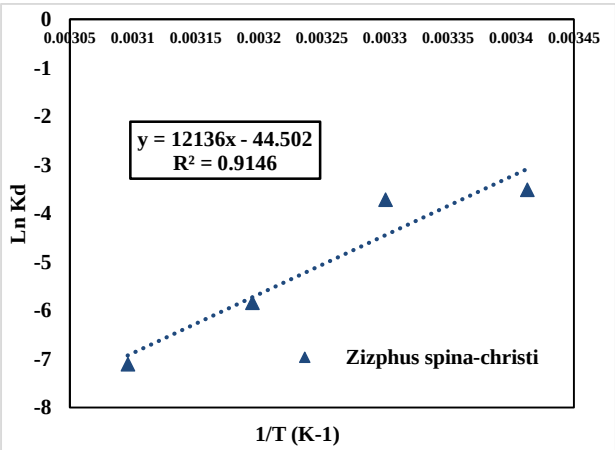

Figure 10. Plot of Ln K_d verse 1/T (K^{-1}) of MO adsorption on ZSCP.

Table 3. Thermodynamic parameters of MO adsorption on ZSCP.

T (K)	ΔGº (kJ/mole)	K_d (g/L)	ΔHº (kJ/mole)	ΔSº (kJ/mole.K)
293	8.568	0.030	-100.933	- 0.370
303	9.369	0.024		
313	15.213	0.003		
323	19.090	0.001		

Conclusion:

In this current work, the effective adsorption of MO on low cost adsorbent (ZSCP) was investigated. ZSCP was found to have a heterogeneous rough surface which provides suitable pore sites for the adsorption of MO molecules. The optimum batch operating parameters with a maximum removal and adsorption capacities were at pH = 2, contact time of 40 min., initial dye concentration of 12 mg/L, adsorbent dosage = 4 g/ 100 ml of dye solution, and temperature of 20 ºC (293 K). The adsorption process of MO on ZSCP followed a pseudo-second order kinetics. D-R isotherm model fitted to the equilibrium data with a maximum adsorption capacity of (4.255 mg/g). The shift towards a positive value of ΔGº as the temperature of the process rises indicated a non-spontaneous and feasible process at lower temperatures that does not require any additional energy. Furthermore, a negative value of both ΔHº and ΔSº indicates an endothermic process where the randomness at the solid-liquid interface decreases during the adsorption process respectively.

Acknowledgment:

This research was financially and technically supported by the Biology Department, Al-Rasheed University College

Author's declaration:

- Conflicts of Interest: None.
- I hereby confirm that all the Figures and Tables in the manuscript are mine. Besides, the Figures and images, which are not mine, have been given the permission for re-publication attached with the manuscript.
- Ethical Clearance: The project was approved by the local ethical committee in Al-Rasheed University College.

References:

1. Bulgariu L, Escudero LB, Bello OS, Iqbal M, Nisar J, Adegoke KA, et al. The utilization of leaf-based adsorbents for dyes removal: A review. J Mol Liq .

2019; 276: 728-47 doi:https://doi.org/10.1016/j.molliq.2018.12.001
2. Kadhom M, Albayati N, Alalwan H, Al-Furaiji M. Removal of dyes by agricultural waste. Sustain Chem Pharm. 2020; 16: 100259 doi:https://doi.org/10.1016/j.scp.2020.100259
3. Ahmad A, Khan N, Giri BS, Chowdhary P, Chaturvedi P. Removal of methylene blue dye using rice husk, cow dung and sludge biochar: Characterization, application, and kinetic studies. Bioresour Technol. 2020; 306: 123202 doi:https://doi.org/10.1016/j.biortech.2020.123202
4. Xia L, Zhou S, Zhang C, Fu Z, Wang A, Zhang Q, et al. Environment-friendly Juncus effusus-based adsorbent with a three-dimensional network structure for highly efficient removal of dyes from wastewater. J Clean Prod. 2020; 259: 120812 doi:https://doi.org/10.1016/j.jclepro.2020.120812
5. Zhang F, Tang X, Huang Y, Keller AA, Lan J. Competitive removal of Pb2+ and malachite green from water by magnetic phosphate nanocomposites. Water Res. 2019; 150: 442-51 doi:https://doi.org/10.1016/j.watres.2018.11.057
6. Abu Elella MH, ElHafeez EA, Goda ES, Lee S, Yoon KR. Smart bactericidal filter containing biodegradable polymers for crystal violet dye adsorption. Cellulose. 2019; 26(17): 9179-206 doi:https://doi.org/10.1007/s10570-019-02698-1
7. Khatri J, Nidheesh PV, Anantha Singh TS, Suresh Kumar M. Advanced oxidation processes based on zero-valent aluminium for treating textile wastewater. Chem Eng J. 2018; 348: 67-73 doi:https://doi.org/10.1016/j.cej.2018.04.074
8. Obiora-Okafo IA, Onukwuli OD. Characterization and optimization of spectrophotometric colour removal from dye containing wastewater by Coagulation-Flocculation. Pol J Chem Technol. 2018; 20(4): 49-59 doi:https://doi.org/10.2478/pjct-2018-0054
9. Li C, Zhang M, Song C, Tao P, Sun M, Shao M, et al. Enhanced Treatment Ability of Membrane Technology by Integrating an Electric Field for Dye Wastewater Treatment: A Review. J AOAC Int. 2018; 101(5): 1341-52 doi:https://doi.org/10.5740/jaoacint.18-0050
10. Nwodika C, Onukwuli Do. Adsorption study of kinetics and equilibrium of basic dye on kola nut pod carbon. Gazi Univ J Sci. 2017;30(4):86-102
11. Abate GY, Alene AN, Habte AT, Getahun DM. Adsorptive removal of malachite green dye from aqueous solution onto activated carbon of Catha edulis stem as a low cost bio-adsorbent. Environ Syst Res. 2020; 9(1): 29 doi:https://doi.org/10.1186/s40068-020-00191-4
12. Boudechiche N, Fares M, Ouyahia S, Yazid H, Trari M, Sadaoui Z. Comparative study on removal of two basic dyes in aqueous medium by adsorption using activated carbon from Ziziphus lotus stones. Microchem J 2019; 146: 1010-8 doi:https://doi.org/10.1016/j.microc.2019.02.010
13. Zhang P, O'Connor D, Wang Y, Jiang L, Xia T, Wang L, et al. A green biochar/iron oxide composite for methylene blue removal. J Hazard Mater. 2020; 384: 121286 doi:https://doi.org/10.1016/j.jhazmat.2019.121286
14. Ragab A, Ahmed I, Bader D. The Removal of Brilliant Green Dye from Aqueous Solution Using Nano Hydroxyapatite/Chitosan Composite as a Sorbent. Molecules. 2019; 24(5) doi:10.3390/molecules24050847
15. Gouamid M, Ouahrani MR, Bensaci MB. Adsorption Equilibrium, Kinetics and Thermodynamics of Methylene Blue from Aqueous Solutions using Date Palm Leaves. Energy Procedia. 2013; 36: 898-907 doi:https://doi.org/10.1016/j.egypro.2013.07.103
16. Inyinbor A, Adekola F, Olatunji GA. Kinetics, isotherms and thermodynamic modeling of liquid phase adsorption of Rhodamine B dye onto Raphia hookerie fruit epicarp. Water Resour Ind. 2016; 15: 14-27 doi:https://doi.org/10.1016/j.wri.2016.06.001
17. Ekrami E, Dadashian F, Arami M. Adsorption of methylene blue by waste cotton activated carbon: equilibrium, kinetics, and thermodynamic studies. Desalination Water Treat. 2016; 57(15): 7098-108 doi:https://doi.org/10.1080/19443994.2015.1015173
18. Wang L, Chen Z, Wen H, Cai Z, He C, Wang Z, et al. Microwave assisted modification of activated carbons by organic acid ammoniums activation for enhanced adsorption of acid red 18. Powder Technol. 2018; 323: 230-7 doi:https://doi.org/10.1016/j.powtec.2017.10.021
19. Ragab A, Ahmed I, Bader D. The Removal of Brilliant Green Dye from Aqueous Solution Using Nano Hydroxyapatite/Chitosan Composite as a Sorbent. Molecules. 2019;24(5):847 doi: https://doi.org/10.3390/molecules24050847
20. Ahmad MA, Ahmad Puad NA, Bello OS. Kinetic, equilibrium and thermodynamic studies of synthetic dye removal using pomegranate peel activated carbon prepared by microwave-induced KOH activation. Water Resour Ind. 2014; 6: 18-35 doi:https://doi.org/10.1016/j.wri.2014.06.002
21. Aljeboree AM, Alshirifi AN, Alkaim AF. Kinetics and equilibrium study for the adsorption of textile dyes on coconut shell activated carbon. Arab J Chem. 2017; 10: S3381-S93 doi:https://doi.org/10.1016/j.arabjc.2014.01.020
22. Zhao P, Zhang R, Wang J. Adsorption of methyl orange from aqueous solution using chitosan/diatomite composite. Water Sci Technol. 2017; 75(7): 1633-42 doi:https://doi.org/10.2166/wst.2017.034
23. Sumanjit, Rani S, Mahajan RK. Equilibrium, kinetics and thermodynamic parameters for adsorptive removal of dye Basic Blue 9 by ground nut shells and Eichhornia. Arab J Chem. 2016; 9: S1464-S77 doi:https://doi.org/10.1016/j.arabjc.2012.03.013
24. Jawad AH, Ngoh Y, Radzun KA. Utilization of watermelon (Citrullus lanatus) rinds as a natural low-cost biosorbent for adsorption of methylene blue: kinetic, equilibrium and thermodynamic studies. J Taibah Univ Sci J. 2018; 12(4): 371-81 doi:https://doi.org/10.1080/16583655.2018.1476206

25. Jawad AH, Rashid RA, Ishak MAM, Ismail K. Adsorptive removal of methylene blue by chemically treated cellulosic waste banana (Musa sapientum) peels. J Taibah Univ Sci J. 2018; 12(6): 809-19 doi:https://doi.org/10.1080/16583655.2018.1519893
26. Saha PD, Chakraborty S, Chowdhury S. Batch and continuous (fixed-bed column) biosorption of crystal violet by Artocarpus heterophyllus (jackfruit) leaf powder. Colloids Surf B. 2012; 92: 262-70 doi:https://doi.org/10.1016/j.colsurfb.2011.11.057
27. Jain SN, Gogate PR. Adsorptive removal of acid violet 17 dye from wastewater using biosorbent obtained from NaOH and H2SO4 activation of fallen leaves of Ficus racemosa. J Mol Liq. 2017; 243: 132-43 doi:https://doi.org/10.1016/j.molliq.2017.08.009
28. Wong S, Tumari HH, Ngadi N, Mohamed NB, Hassan O, Mat R, et al. Adsorption of anionic dyes on spent tea leaves modified with polyethyleneimine (PEI-STL). J Clean Prod. 2019; 206: 394-406 doi:https://doi.org/10.1016/j.jclepro.2018.09.201
29. Ahmaruzzaman M. Removal of Methyl Orange from Aqueous Solution Using Activated Papaya Leaf. Sep Sci Technol. 2012; 47(16): 2381-90
30. Wong S, Tumari HH, Ngadi N, Mohamed NB, Hassan O, Mat R, et al. Adsorption of anionic dyes on spent tea leaves modified with polyethyleneimine (PEI-STL). J Clean Prod. 2019; 206: 394-406 doi:https://doi.org/10.1016/j.jclepro.2018.09.201
31. Krika F, Benlahbib OeF. Removal of methyl orange from aqueous solution via adsorption on cork as a natural and low-coast adsorbent: equilibrium, kinetic and thermodynamic study of removal process. Desalination Water Treat. 2015; 53(13): 3711-23 doi:https://doi.org/10.1080/19443994.2014.995136
32. Bhattacharyya KG, Sharma A. Azadirachta indica leaf powder as an effective biosorbent for dyes: a case study with aqueous Congo Red solutions. J Environ Manage. 2004; 71(3): 217-29 doi:https://doi.org/10.1016/j.jenvman.2004.03.002
33. Rattanapan S, Srikram J, Kongsune P. Adsorption of Methyl Orange on Coffee grounds Activated Carbon. Energy Procedia. 2017; 138: 949-54 doi:https://doi.org/10.1016/j.egypro.2017.10.064
34. Mizhir AA, Al-Lami HS, Abdulwahid AA. Kinetic, Isotherm, and Thermodynamic Study of Bismarck Brown Dye Adsorption onto Graphene Oxide and Graphene Oxide-Grafted-Poly (n-butyl methacrylate-co-methacrylic Acid). Baghdad Sci J. 2022; 19(1): 0132 doi:https://doi.org/10.21123/bsj.2022.19.1.0132
35. Mousa SA, Tareq S, Muhammed EA. Studying the Photodegradation of Congo Red Dye from Aqueous Solutions Using Bimetallic Au–Pd/TiO2 Photocatalyst. Baghdad Sci J. 2021; 18(4): 1261 doi:https://doi.org/10.21123/bsj.2021.18.4.1261

دراسة توازن حركية و ثرمودنامكية لازالة صبغة المثيل البرتقالي من المحلول المائي باستخدام مطحون ورق نبات السدر

فادية فالح محمد

قسم علوم الحياة، كلية الرشيد الجامعة، بغداد، العراق.

الخلاصة:

تم في هذه الدراسة استخدام مطحون ورق السدر لامتزاز صبغة المثيل البرتقالي. حيث تمت دراسة تاثير كل من الرقم الحامضي (2-12), زمن التلامس (0-60 دقيقة), التركيزالابتدائي للصبغة (2-20 ملغم/ل), كمية المادة الممتزة (0-4.5 غم) و تاثير درجة الحرارة (20-50 سº) على عملية الامتزاز. اظهرات النتائج الحصول على اقصى معدل للامتزاز و سعة امتزاز (ملغم /غم = q_e ,R=23.146% 2.778) عند رقم حامضي = 2 حيت تم الوصول الى نقطة التوازن بعد 40 دقيقة. وجد ان حركية الدرجة الثانية الزائفة هي اكثر ملائمة للتعبير عن حركية الامتزاز (R^2= 0.997). اخضعت النتائج المختبرية الى اربع نماذج ايزوثيرم مختلفة (لانكمايروفريندليش ودوبيين رادوشكيفيش وتيمكن) ووجد أن عملية الامتزاز تلائم دوبيين رادوشكيفيش ايزوثيرم (R^2=0.970). دراسة الخصائص الثرموديناميكية ,ΔGº (ΔHº, ΔSº) لعملية الامتزاز اظهرت ان العملية غير تلقائية ,باعثة للحرارة, و قابلة للتنفيذ عند درجات تشغيلية واطئة (كيلو جول/مول ΔHº = -100.933) مع انخفاض في العشوائية على الجبهه الفاصلة بين المادة الصلبة و الوسط المائي (كيلو جول /مول.كلفن - = ΔSº 0.370)

الكلمات المفتاحية: امتزاز, دوبيين رادوشكيفيش ايزوثيرم, المثيل البرتقالي, حركية الدرجة الثانية الكاذبة, الخصائص الثرموديناميكية, مطحون ورق نبات السدر.